

# Tetrapyridine and Tetrapyrazine TTF Derivatives: Synthesis, Characterization and Preparation of a Bimetallic Co<sup>II</sup> Complex

Sandra I. G. Dias,<sup>[a]</sup> Ana I. S. Neves,<sup>[a]</sup> Sandra Rabaça,<sup>[a]</sup> Isabel C. Santos,<sup>[a]</sup> and Manuel Almeida\*<sup>[a]</sup>

**Keywords:** Electron donors / Tetrathiafulvalene / Nitrogen ligands / Cobalt / Magnetic studies

The tetra-substituted TTF-type donors 4,4',5,5'-tetrakis(2-pyridylethylsulfanyl)tetrathiafulvalene (**1**) and 4,4',5,5'-tetrakis(2-pyrazylethylsulfanyl)tetrathiafulvalene (**2**) were prepared and characterized. These donors show a redox behaviour that is comparable with similar unsubstituted TTF donors, with a small increase of the redox potentials due to the electron-withdrawing effect of the pyridine and pyrazine groups. Single crystal X-ray diffraction analyses show structures with a strong segregation of TTF and azo moieties. The

pyridine-substituted donor **1** was used as a bridging ligand to prepare a dinuclear Co<sup>II</sup>-coordination complex [1Co<sub>2</sub>(hfac)<sub>4</sub>] (hfac = hexafluoroacetylacetonate) with redox properties identical to that of **1**. This dinuclear complex presents an effective magnetic moment of ca. 8 μ<sub>B</sub>, corresponding to nearly independent *S* = 3/2 spins with weak antiferromagnetic interactions below 65 K.

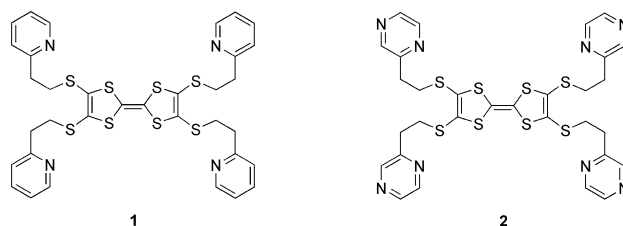
(© Wiley-VCH Verlag GmbH & Co. KGaA, 69451 Weinheim, Germany, 2008)

## Introduction

One of the current challenges in molecular materials is the preparation of multifunctional materials combining conducting and magnetic properties in a synergetic manner. An established strategy for the preparation of such multifunctional molecular materials is the combination of electro-active molecules that are suitable for making conducting networks, in the solid state, when partially oxidized with paramagnetic counterions. Indeed, in the past years this strategy has led to materials exhibiting novel properties resulting for instance from the coexistence of conducting and magnetic chains with an interplay between their instabilities,<sup>[1]</sup> leading to paramagnetic conductors and superconductors<sup>[2]</sup>, or even to ferromagnetic superconductors<sup>[3]</sup>, or field-induced superconductors.<sup>[4]</sup> However, for all these compounds the interaction between conducting π electrons and localized magnetic moments of d electrons, the so-called π–d interaction, was found to be rather weak.

An alternative approach to realise the π–d interaction is to use coordination bonds to directly attach an electro-active molecule to paramagnetic transition metals. Following this strategy, several tetrathiafulvalene (TTF) derivatives bearing functional groups that can coordinate to transition metals, especially the N-containing groups,<sup>[5]</sup> along with some transition-metal complexes have already been reported during the last years.<sup>[6]</sup> To the best of our knowledge

this type of transition-metal complex, coordinated by N atoms, has been obtained with asymmetrically substituted TTF ligands. In this paper we describe the synthesis of members of a new series of tetrapyridine- and tetrapyrazine-substituted TTF donors, **1** and **2**, as well as the preparation and characterization of a new dinuclear Co<sup>II</sup>-coordination complex of **1**, acting as a bridging ligand with hfac as the capping ligands [1Co<sub>2</sub>(hfac)<sub>4</sub>] (hfac = hexafluoroacetylacetonate). We thus demonstrate the possible use of the donors **1** and **2** in preparing polynuclear complexes.



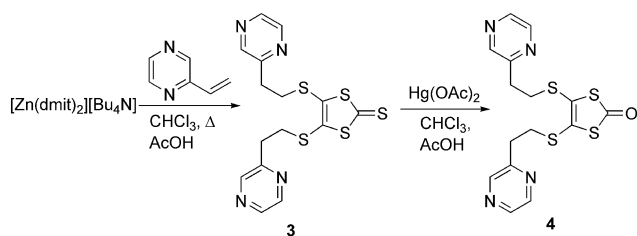
## Results and Discussion

Compound 4,5-bis(2-pyrazylethylsulfanyl)-1,3-dithiole-2-thione (**3**) has been prepared by the direct reaction of the zinc salt of dmit<sup>2-</sup>, [Zn(dmit)<sub>2</sub>][Et<sub>4</sub>N]<sub>2</sub>, with 2-vinylpyrazine in chloroform/acetic acid (3:1) in 67% yield.<sup>[7]</sup> The treatment of compound **3** with mercury acetate afforded 4,5-bis(2-pyrazylethylsulfanyl)-1,3-dithiole-2-one (**4**) in 46% yield as depicted in Scheme 1.

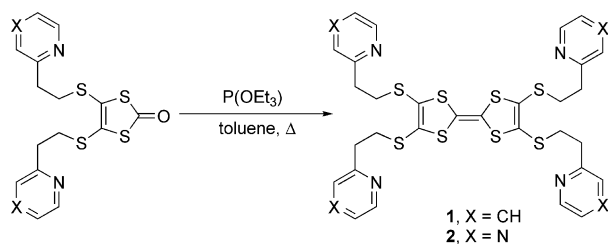
The TTF derivatives 4,4',5,5'-tetrakis(2-pyridylethylsulfanyl)tetrathiafulvalene (**1**) and 4,4',5,5'-tetrakis(2-pyrazylethylsulfanyl)tetrathiafulvalene (**2**) were obtained from

[a] Dept. Química, Instituto Tecnológico e Nuclear / CFMCL, Estrada Nacional 10, 2686-953 Sacavém, Portugal  
Fax: +351-219-941455  
E-mail: malmeida@itn.pt

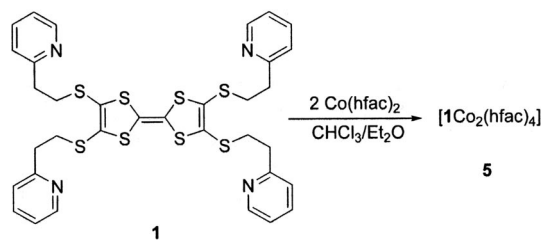
Supporting information for this article is available on the WWW under <http://www.eurjic.org> or from the author.

Scheme 1. Synthesis of thione **3** and ketone **4**.

the phosphite-mediated homo-coupling of the corresponding 1,3-dithiole-2-one in 29% and 28% yield, respectively (Scheme 2). All compounds have been characterized by  $^1\text{H}$  NMR and  $^{13}\text{C}$  NMR spectroscopy as well as a CHNS analysis, and the results confirm their purity and composition. Suitable single crystals for X-ray diffraction analyses of compounds **1**, **2** and **3** and a full structural refinement were obtained.

Scheme 2. Synthesis of the TTF derivatives **1** and **2**.

Complex  $[\text{Co}_2(\text{hfac})_4]$  (**5**) was obtained by treating the electron donor **1** with a twofold amount of  $[\text{Co}(\text{hfac})_2]$  in a  $\text{CHCl}_3/\text{Et}_2\text{O}$  solution (Scheme 3). Suitable single crystals for an X-ray diffraction analysis were obtained by slow diffusion of the solution of reagents at room temperature. It is worth mentioning that there are a few similar cases of bimetallic complexes that have TTF derivatives with phosphane-coordinating groups as bridging ligands,<sup>[8]</sup> but to the best of our knowledge this is the first of such bimetallic complexes based on a TTF derivative with nitrogen-coordination groups.

Scheme 3. Synthesis of the  $\text{Co}^{\text{II}}$  complex **5**.

The redox potentials of the new electron donors **1** and **2** and also the coordination complex **5** were measured by cyclic voltammetry (CV). The CV data are collected in Table 1. For comparison, the oxidation potential of BEDT-TTF and 4,4',5,5'-tetrakis(4-picolylthio)tetrathiafulvalene (PT-TTF)<sup>[5a]</sup> are also included in Table 1. In each case two single-electron oxidation waves are observed for the new

electron donors, corresponding to the sequential formation of the stable TTF-radical cation and the dication, as expected for TTF-based derivatives. While these waves are clearly reversible for **2**, a slightly larger separation between anodic and cathodic peaks are observed in **1**. Compared to BEDT-TTF, the attachment of the pyridine and pyrazine units mainly increases the first redox wave potential due to the electron-withdrawing effect of the pyridine and pyrazine units.<sup>[9]</sup> Because of solubility issues the CV data of complex **5** were collected using THF as the solvent, and for comparison purposes the values of **1** in THF are also presented in Table 1. Coordination of the  $\text{Co}^{\text{II}}$  ion does not significantly change the redox potentials.

Table 1. Oxidation potentials of compounds **1**, **2** and **5** measured by cyclic voltammetry.<sup>[a]</sup>

Compound	$E^1_{1/2}$ [V]	$E^2_{1/2}$ [V]
<b>1</b>	0.56 (0.56) <sup>[b]</sup>	0.89 (0.74) <sup>[b]</sup>
<b>2</b>	0.60	0.90
<b>5</b>	0.61 <sup>[b]</sup>	0.80 <sup>[b]</sup>
BEDT-TTF <sup>[5a]</sup>	0.49	0.89
PT-TTF <sup>[5a]</sup>	0.50	0.88

[a] Conditions: oxidation potentials were determined in  $\text{CH}_2\text{Cl}_2$  at room temperature containing 0.1 M  $\text{Bu}_4\text{NPF}_6$ , with  $\text{Ag}/\text{AgCl}$  as the reference electrode and Pt as the working electrode; scan rate is  $100 \text{ mV s}^{-1}$ . [b] In THF.

We sought to obtain X-ray diffraction quality crystals in order to gain more insight into the structure and the crystal packing of the new compounds. Suitable single crystals of **1**, **3** and **5** were obtained by diffusion techniques. Selected bond lengths are shown in Table 2. Their crystallographic and structural refining data are listed in Table 3 in the Exp. Section.

Table 2. Selected bond lengths [ $\text{\AA}$ ].

Compound	<b>1</b>	<b>3</b>	<b>5</b>
S(1)–C(1)	1.7604(19)	1.6386(17)	1.761(3)
S(1)–C(2)	1.7631(19)	1.7447(17)	1.751(4)
S(2)–C(1)	1.755(2)	1.7268(17)	1.759(4)
S(2)–C(3)	1.7622(19)	1.7473(16)	1.756(4)
S(3)–C(2)	1.7506(19)	1.7476(17)	1.748(4)
S(3)–C(4)	1.821(2)	1.8132(17)	1.819(4)
S(4)–C(3)	1.7546(19)	1.7431(16)	1.748(4)
S(4)–C(11)	1.794(4)	1.8278(17) <sup>[a]</sup>	1.810(4)
S(4)–C(18)	1.793(4)		
S(5)–C(1)		1.6490(17)	
C(1)–C(1*)	1.337(4)		1.325(7)

[a] S(4)–C(10).

Compound **3** crystallizes in the triclinic system, space group  $P\bar{1}$  with two identical molecules in the unit cell. An ORTEP plot of molecule **3** with the atom numbering scheme is shown in Figure 1. Molecule **3** contains an essentially planar moiety, comprising atoms C(1), C(2), C(3) and all five sulfur atoms (Rms deviation of fitted atoms =  $0.0303 \text{ \AA}$ ). The pyrazine rings form dihedral angles of  $76.91(3)^\circ$  and  $15.63(8)^\circ$  with the mean plane of the central part of the molecule. The two pyrazine rings make a dihedral angle of  $79.65(5)^\circ$  with each other.

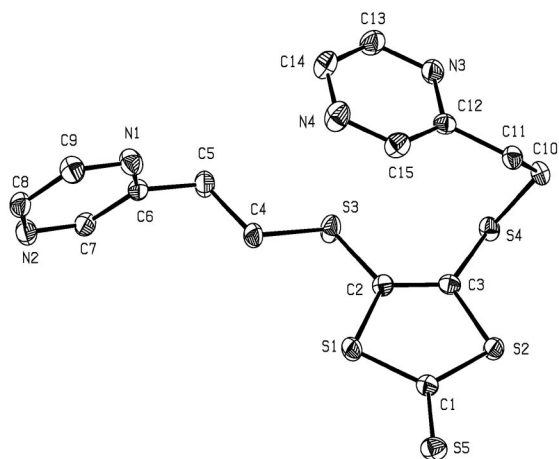


Figure 1. ORTEP diagram of compound **3** drawn at the 40% probability level and showing the atomic numbering scheme. H atoms have been omitted for clarity.

The structure of TTF derivative **1**, obtained as orange single crystals from a mixture of solvents (toluene/hexane), was solved by X-ray diffraction analysis. It crystallizes in the monoclinic system, space group  $C2/c$  with an inversion centre at the TTF double bond. Figure 2 shows an ORTEP plot of **1** and the atomic numbering employed. The central part of the molecule comprising the central TTF core and the thioether S atoms [C(1), C(2), C(3), S(1), S(2), S(3), S(4)] is essentially planar (Rms deviation of fitted atoms: 0.040 Å). While the ethyl-pyridine groups deviate from the central plane. One of the pyridine rings is disordered over two sites with an occupancy of 50:50. The dihedral angles between the pyridine rings and the TTF mean plane are 85.12(2)° and 60.42(2)° or 66.67(2)°.

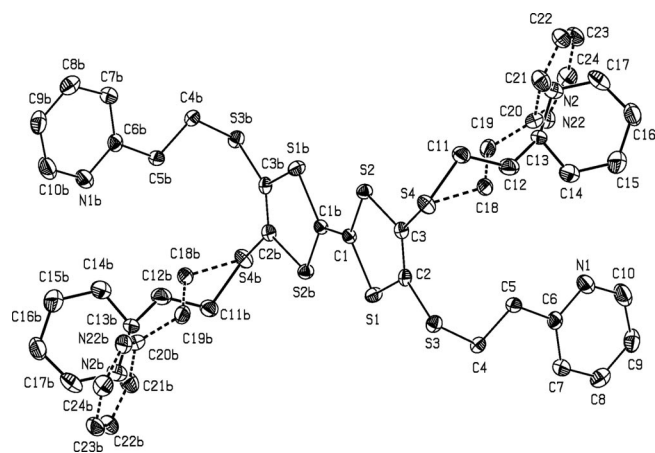


Figure 2. ORTEP diagram of compound **1** drawn at the 40% probability level and showing the atomic numbering scheme. H atoms have been omitted for clarity.

The crystal structure of **1** contains donor stacks along the  $b$  plane (Figure 3). The TTF units stack on top of each other with a large displacement along the transverse axis due to the pyridine groups. The shorter intrastack contact occurs between S(2)–S(2\*) at 3.626(1) Å ( $-x + 0.5, -y +$

0.5,  $-z + 2$ ) and C(1)–S(4\*) at 3.494(2) Å ( $x, y - 1, z$ ). As shown in Figure 3 the structure is seen to be made up of layers, parallel to the  $b,c$  plane, of TTF groups alternating along the  $a$  plane with layers of pyridine moieties.

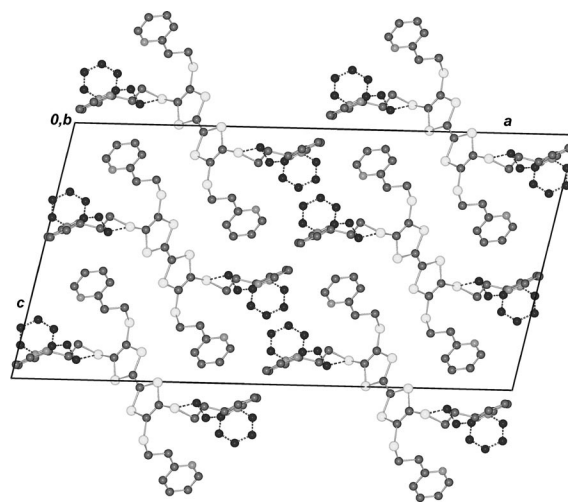


Figure 3. View of the crystal structure of compound **1** along the  $b$  plane. Hydrogen atoms have been omitted for clarity. One of the disordered pyridine rings is represented by dashed lines.

Although the quality of the crystal of compound **2** was poor and the structure refinement of low quality, it enabled us to unambiguously identify its molecular structure and crystal packing. The TTF derivative **2** crystallizes in the triclinic system, space group  $P\bar{1}$  with cell parameters  $a = 5.5879(11)$  Å,  $b = 8.4827(18)$  Å,  $c = 17.872(4)$  Å,  $\alpha = 79.003(12)^\circ$ ,  $\beta = 84.401(12)^\circ$ ,  $\gamma = 79.476(12)^\circ$ ,  $V = 815.9(3)$  Å<sup>3</sup>. The molecular structure of **2** is shown in Figure 4 and it contains a planar moiety comprising of the central TTF core and all the S atoms [C(1), C(2), C(3), S(1), S(2), S(3), S(4)] (Rms = 0.0544 Å). As expected, the pyrazine rings deviate from the central TTF plane with dihedral angles of 50.06(54)° and 75.42(42)°. The two pyrazine rings make a dihedral angle of 67.23(61)°. In a similar manner to **1**, the crystal structure of this donor presents a clear segregation of TTF and pyrazine moieties in alternating layers.

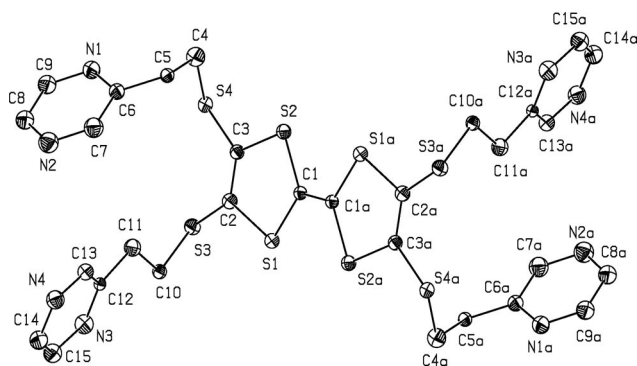


Figure 4. ORTEP diagram of compound **2** drawn at the 40% probability level and showing the atomic numbering scheme. H atoms have been omitted for clarity.

Complex **5** crystallizes in the centrosymmetric  $P\bar{1}$  space group, with the inversion centre lying in the middle of the central C=C bond of the TTF moiety. Figure 5 shows an ORTEP plot of **5** and the atomic numbering employed. The TTF core is slightly deviated from planarity (Rms deviation of fitted atoms = 0.1017 Å). The cobalt atom is coordinated to the nitrogen atoms of the two adjacent pyridine rings and two hfac molecules in the *cis* position. As is often observed for hfac ligands, one of the CF<sub>3</sub> groups is highly disordered.<sup>[6,10]</sup> The cobalt atoms have an octahedral coordination with the O(1), O(2), O(3), O(4), N(1) and N(2) atoms. The O(1) and N(2) atoms are in the apical positions at 174.83(11)°. The Co...O and Co...N bond lengths are in the usual range for Co<sup>II</sup> complexes.<sup>[11]</sup> The bond lengths and bond angles of the TTF core are within experimental uncertainty and equal to those of the uncoordinated donor **1**, indicating that the TTF ligand remains in the neutral state (Table 2). This includes the central C=C bond, particularly sensitive to the oxidation state of TTF donors, presenting a value of 1.325(7) Å, typical of a neutral donor.<sup>[12]</sup>

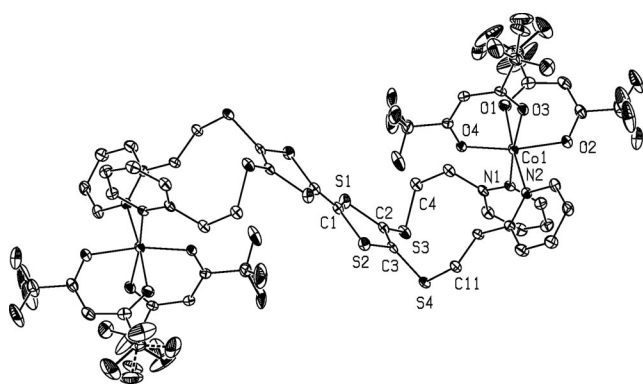


Figure 5. ORTEP diagram of complex **5** at the 50% probability level and showing the atomic numbering scheme. H atoms have been omitted for clarity.

The crystal packing of **5** (Figure 6) presents a segregation of TTF cores and Co-coordination groups in alternating layers parallel to the *a,b* plane. The TTF groups are connected by short contacts C(3)–S(4\*) at 3.430(3) Å ( $-x + 1, -y, -z + 1$ ) along the columns and with the side columns S(3)–S(3\*) at 3.462(1) Å ( $-x, -y, -z + 1$ ). Each Co atom has eight other Co atoms as next neighbours at distances that are in the range 8.9–12.9 Å, smaller than the intramolecular Co–Co distance of 14.638(2) Å.

The temperature-dependent magnetic susceptibility of complex **5** was measured over the range 3–300 K. Figure 7 displays the effective magnetic moment  $\mu_{\text{eff}}$  vs. temperature plot. At room temperature the effective magnetic moment is 8  $\mu_{\text{B}}$ , it increases slightly upon cooling, reaching a broad maximum of 8.4  $\mu_{\text{B}}$  around 65 K and finally decreases below 60 K as shown in Figure 7. The high temperature effective magnetic moment is close to the expected value for two  $S = 3/2$  non-interacting spins, one in each Co<sup>II</sup> atom with  $g = 2.92$  (8.00  $\mu_{\text{B}}$ ).<sup>[13]</sup> This compound was found to be EPR

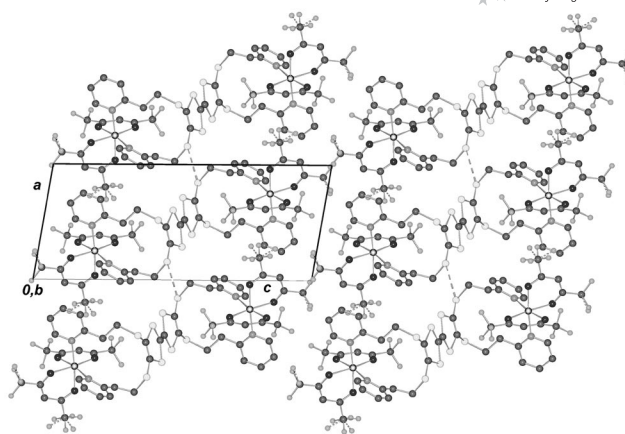


Figure 6. View of the crystal packing arrangement of compound **5** along the *b* plane. H atoms have been omitted for clarity. Dashed lines show the short contacts between S(3)–S(3\*) at 3.462(1) Å ( $-x, -y, -z + 1$ ).

silent and therefore this deduced *g* value could not be confirmed, but it is in the typical range for similar Co<sup>II</sup> complexes.

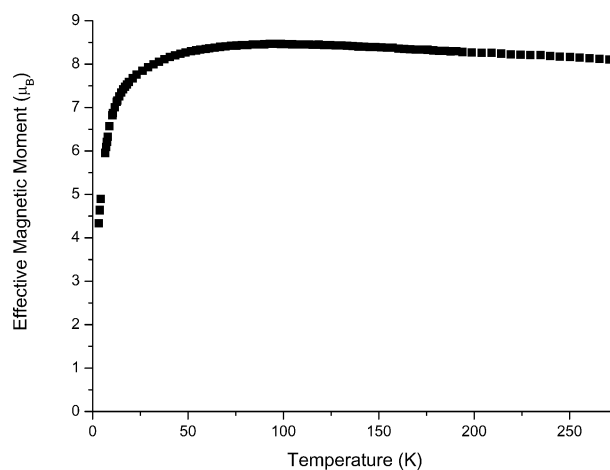


Figure 7. Effective magnetic moment vs. temperature plot for complex **5**.

The small increase of  $\mu_{\text{eff}}$  upon cooling from room temperature may be attributed to an additional angular contribution of cobalt spins as found in other bimetallic complexes.<sup>[13]</sup> The decrease of  $\mu_{\text{eff}}$  below 60 K denotes antiferromagnetic interactions and the magnetic susceptibility in the range 65–10 K can be fairly well fitted to a Curie–Weiss model with  $\theta = -6.9$  K. These antiferromagnetic interactions can either be intramolecular or intermolecular. In fact each Co atom, besides being connected through the ligand to another Co atom at a distance of 14.6 Å, has an additional eight neighbouring Co atoms at distances in the range 8.9–12.9 Å. The intermolecular interactions although at shorter distances are not necessarily larger than the intramolecular interaction through the TTF groups. However, the latter, probably because of the lack of conjugation from pyridine to pyridine rings, is not dominant and certainly

not significant since a simple model of antiferromagnetically coupled  $S = 3/2$  dimers is unable to properly fit the data.

## Conclusions

We described the synthesis of new tetrapyrroline- and tetrapyrazine-substituted TTFs with donor properties that are suitable for use as electro-active species in the preparation of conducting materials. Their electrochemical behaviour and crystal structure were determined by cyclic voltammetry and X-ray diffraction analyses. With the preparation and characterization of a dinuclear  $\text{Co}^{\text{II}}$ -coordination complex, with the tetrapyrroline TTF donor acting as a bridging ligand, we demonstrate the possible use of these tetra-substituted TTF-type donors as ligands in preparing bimetallic complexes. These results open the way, presently being further explored by us, to prepare similar complexes with other metals and to achieve even more complex coordination architectures.

## Experimental Section

**General Remarks:** All solvents were purified following standard procedures.  $[\text{Zn}(\text{dmit})_2][\text{Et}_4\text{N}]_2$  and 4,5-bis(2-pyridylethylsulfanyl)-1,3-dithiole-2-one were prepared by literature methods.<sup>[14,15]</sup> Other chemicals were commercially obtained and used without further purification. Column chromatography was carried out using silica gel ( $0.063 \pm 0.2$  mm). IR spectra were obtained with a Shimadzu FTIR-8400S. Melting points were obtained with a Stuart Scientific SMP2. CHNS analyses were performed with a Carlo Erba apparatus.  $^1\text{H}$  and  $^{13}\text{C}$  NMR spectra were recorded with a Bruker Aspect 3000 (300 MHz for  $^1\text{H}$ ) with  $\text{CDCl}_3$  as a solvent using TMS as the internal reference. Cyclic voltammetry data were obtained using a BAS C3 cell stand at room temperature in  $\text{CH}_2\text{Cl}_2$  and THF that contained  $n\text{Bu}_4\text{PF}_6$  ( $10^{-1}$  M) as the supporting electrolyte, with a scan rate of 100 mV/s, platinum wire working and counter electrodes and a Ag/AgCl reference electrode.

**4,4',5,5'-Tetrakis(2-pyridylethylsulfanyl)tetrathiafulvalene (1):** 4,5-Bis(2-pyridylethylsulfanyl)-1,3-dithiole-2-one (0.9 g, 2.2 mmol) was dissolved in dried toluene (25 mL) under  $\text{N}_2$ . The solution was heated under reflux before the addition of dried  $\text{P}(\text{OEt})_3$  (2.5 mL). This solution was left at reflux overnight under  $\text{N}_2$ . The orange solution was cooled to room temperature, and the orange precipitate was collected by filtration and washed with cold toluene. Compound **1** was isolated as an orange precipitate (0.2 g, 29% yield). X-ray quality crystals were obtained from the slow diffusion of hexane to a toluene solution; m.p. 104 °C.  $\text{C}_{34}\text{H}_{32}\text{N}_4\text{S}_8$  (753.17): calcd. C 54.22, H 4.28, N 7.44, S 34.06; found C 54.17, H 4.06, N 7.66, S 33.46.  $^1\text{H}$  NMR (300 MHz,  $\text{CDCl}_3$ ):  $\delta = 3.14$  (t,  $J = 6.9$  Hz, 8 H,  $-\text{CH}_2$ ), 3.26 (t,  $J = 6.9$  Hz, 8 H,  $-\text{SCH}_2$ ), 7.14 (t,  $J = 4.8$ , 2.4 Hz, 4 H, H5), 7.21 (d,  $J = 7.8$  Hz, 4 H, H3), 7.62 (dt,  $J = 7.5$ , 1.8 Hz, 4 H, H4), 8.53 (dd,  $J = 1.2$ , 4.8 Hz, 4 H, H6) ppm.  $^{13}\text{C}$  NMR (75.3 MHz,  $\text{CDCl}_3$ ):  $\delta = 35.5$ , 38.2, 121.6, 123.4, 127.9, 136.4, 149.4, 158.9 ppm. IR (KBr):  $\tilde{\nu} = 2922$  (w), 1666 (m), 1589 (s), 1473 (s), 1433 (s), 883 (m), 771 (s)  $\text{cm}^{-1}$ .

**4,4',5,5'-Tetrakis(2-pyrazylethylsulfanyl)tetrathiafulvalene (2):** Compound **2** was prepared from **4** (0.6 g, 1.5 mmol) by an analogous procedure to that used for **1**. The orange precipitate was puri-

fied by recrystallization from hot methanol (0.3 g, 28%). X-ray quality crystals were obtained from the slow diffusion of hexane into a dichloromethane solution; m.p. 142 °C.  $\text{C}_{28}\text{H}_{28}\text{N}_8\text{S}_8$  (756.13): calcd. C 47.59, H 3.73, N 14.80, S 33.88; found C 46.66, H 3.70, N 15.14, S 33.30.  $^1\text{H}$  NMR (300 MHz,  $\text{CDCl}_3$ ):  $\delta = 3.16$  (t,  $J = 6.9$  Hz, 8 H,  $-\text{CH}_2$ ), 3.28 (t,  $J = 6.9$  Hz, 8 H,  $-\text{SCH}_2$ ), 8.51 (m, 12 H, pyrazine ring) ppm.  $^{13}\text{C}$  NMR (75.3 MHz,  $\text{CDCl}_3$ ):  $\delta = 34.7$ , 35.3, 127.9, 142.8, 144.2, 144.8, 154.5 ppm. IR (KBr):  $\tilde{\nu} = 2921$  (w), 1521 (m), 1409 (s), 1016 (s), 821 (m), 771 (m)  $\text{cm}^{-1}$ .

**4,5-Bis(2-pyrazylethylsulfanyl)-1,3-dithiole-2-thione (3):**  $[\text{Zn}(\text{dmit})_2][\text{Et}_4\text{N}]_2$  (2.65 g, 3.70 mmol) and 2-vinylpyrazine (2.4 g, 23 mmol) in  $\text{CHCl}_3/\text{AcOH}$  (3:1, 50 mL) were heated under reflux overnight. After cooling to room temperature the precipitate was filtered and washed with water (100 mL), a saturated aqueous solution of  $\text{NaHCO}_3$  ( $2 \times 50$  mL), a saturated aqueous solution of  $\text{NaCl}$  (100 mL) and  $\text{H}_2\text{O}$  (100 mL) and then dried ( $\text{MgSO}_4$ ). After removal of the solvent, column chromatography of the crude reaction mixture on silica gel with ethyl acetate afforded **3** as an orange solid (1.0 g, 67%). Crystals suitable for X-ray diffraction analysis were obtained by slow diffusion of hexane into a chloroform solution; m.p. 81 °C.  $\text{C}_{15}\text{H}_{14}\text{N}_4\text{S}_5$  (409.98): calcd. C 43.87, H 3.44, N 13.64, S 39.05; found C 44.25, H 3.29, N 13.49, S 39.04.  $^1\text{H}$  NMR (300 MHz,  $\text{CDCl}_3$ ):  $\delta = 3.17$  (t,  $J = 6.6$  Hz, 4 H,  $-\text{CH}_2$ ), 3.32 (t,  $J = 6.6$  Hz, 4 H,  $-\text{SCH}_2$ ) 8.50 (m, 6 H, pyrazine ring) ppm.  $^{13}\text{C}$  NMR (75.3 MHz,  $\text{CDCl}_3$ ):  $\delta = 35.1$ , 136.2, 143.1, 144.2, 144.8, 153.9, 210.5 ppm. IR (KBr):  $\tilde{\nu} = 2925$  (w), 1522 (m), 1477 (m), 1406 (s), 1053 (s)  $\text{cm}^{-1}$ .

**4,5-Bis(2-pyrazylethylsulfanyl)-1,3-dithiole-2-one (4):**  $\text{Hg}(\text{OAc})_2$  (2.5 g, 7.7 mmol) was added to a solution of **3** (1.0 g, 2.5 mmol) in  $\text{CHCl}_3/\text{AcOH}$  (3:1, 30 mL). The mixture was stirred at room temperature overnight under  $\text{N}_2$ . The mixture was filtered through celite, washed with water (20 mL), a saturated aqueous solution of  $\text{NaHCO}_3$  ( $3 \times 20$  mL) and  $\text{H}_2\text{O}$  (20 mL), and then dried ( $\text{MgSO}_4$ ). After removing the solvent, column chromatography of the crude reaction mixture on silica gel with ethyl acetate afforded **5** as a white solid that was further recrystallized from methanol (0.5 g, 46%); m.p. 63 °C.  $\text{C}_{15}\text{H}_{14}\text{N}_4\text{OS}_4$  (394.01): calcd. C 45.66, H 3.58, N 14.20, S 32.51; found C 46.01, H 3.23, N 14.32, S 33.47.  $^1\text{H}$  NMR (300 MHz,  $\text{CDCl}_3$ ):  $\delta = 3.19$  (m, 4 H,  $-\text{CH}_2$ ), 3.32 (m, 4 H,  $-\text{SCH}_2$ ), 8.50 (m, 6 H, pyrazine ring) ppm.  $^{13}\text{C}$  NMR (75.3 MHz,  $\text{CDCl}_3$ ):  $\delta = 34.9$ , 127.1, 142.8, 144.1, 144.6, 154.0, 189.0 ppm. IR (KBr):  $\tilde{\nu} = 2927$  (w), 1757 (m), 1674 (s), 1487 (s), 1410 (s), 1065 (m), 1018 (s), 889 (s)  $\text{cm}^{-1}$ .

**[ $\text{Co}_2(\text{hfac})_4$ ] (5):**  $\text{Co}(\text{hfac})_2$  (0.05 g, 0.1 mmol) in chloroform (2 mL) was added to a solution of **1** (0.03 g, 0.05 mmol) in chloroform and diethyl ether (1:1, 2 mL). Crystals formed from slow diffusion of the reaction mixture at room temperature after a couple of weeks; m.p. 222 °C.  $\text{C}_{54}\text{H}_{36}\text{Co}_2\text{F}_{24}\text{N}_4\text{O}_8\text{S}_8$  (1699.22): calcd. C 38.13, H 2.12, N 3.29, S 15.06; found C 37.90, H 1.84, N 3.30, S 15.04. IR (KBr):  $\tilde{\nu} = 2347$  (w), 1643 (s), 1487 (m), 1262 (s), 1202 (m), 1143 (s), 677 (m), 587 (m)  $\text{cm}^{-1}$ .

**X-ray Crystallographic Study:** Crystallographic data for compounds **1**, **2**, **3** and **5** were collected on a Bruker AXS APEX CCD area detector diffractometer equipped with an Oxford Cryosystems low-temperature device at 150(2) K in the  $\omega$  and  $\phi$  scans mode. A semi-empirical absorption correction was carried out using the program SADABS.<sup>[16]</sup> Data collection, cell refinement and data reduction were done with the SMART and SAINT programs.<sup>[17]</sup> The structures were solved by direct methods using SIR97<sup>[18]</sup> and refined by full-matrix least-squares methods with the SHELXL97<sup>[19]</sup> program using the winGX software package.<sup>[20]</sup> Non-hydrogen atoms were placed in idealized positions and allowed to refine ri-

Table 3. X-ray crystallographic data for complexes **1**, **3** and **5**.

Compound	<b>1</b>	<b>3</b>	<b>5</b>
Empirical formula	C <sub>34</sub> H <sub>32</sub> N <sub>4</sub> S <sub>8</sub>	C <sub>15</sub> H <sub>14</sub> N <sub>4</sub> S <sub>5</sub>	C <sub>54</sub> H <sub>36</sub> Co <sub>2</sub> F <sub>24</sub> N <sub>4</sub> O <sub>8</sub> S <sub>8</sub>
<i>M<sub>r</sub></i> [g mol <sup>-1</sup> ]	753.12	410.60	1699.21
<i>T</i> [K]	150(2)	150(2)	150(2)
Crystal system	monoclinic	triclinic	triclinic
Space group	<i>C</i> 2/ <i>c</i>	<i>P</i> $\bar{1}$	<i>P</i> $\bar{1}$
<i>a</i> [Å]	35.9346(8)	5.5814(6)	8.8725(3)
<i>b</i> [Å]	5.1212(1)	12.3380(13)	8.9882(4)
<i>c</i> [Å]	18.8356(4)	13.2439(14)	21.1573(9)
$\alpha$ [°]	90	102.698(6)	87.297(2)
$\beta$ [°]	102.6540(10)	94.269(6)	80.261(2)
$\gamma$ [°]	90	99.925(5)	87.851(2)
<i>V</i> [Å <sup>3</sup> ]	3382.09(12)	870.39(16)	1660.34(12)
<i>Z</i>	4	2	1
<i>D</i> <sub>calcd.</sub> [Mg m <sup>-3</sup> ]	1.479	1.567	1.699
$\mu$ [mm <sup>-1</sup> ]	0.561	0.671	0.873
<i>F</i> (000)	1568	424	850
Crystal size [mm]	0.30 × 0.20 × 0.10	0.40 × 0.30 × 0.20	0.24 × 0.20 × 0.04
$\theta$ range [°]	3.49 to 26.37	2.61 to 26.36	2.67 to 25.68
Index range ( <i>h,k,l</i> )	-43/44, -6/6, -23/22	-6/6, -15/15, -16/16	-10/10, -10/10, -25/25
Reflections collected/unique	11535/3440 [R <sub>int</sub> = 0.0567]	8661/3540 [R <sub>int</sub> = 0.0424]	11183/6281 [R <sub>int</sub> = 0.0427]
<i>T</i> <sub>max</sub> , <i>T</i> <sub>min</sub>	0.9460, 0.8497	0.8775, 0.7752	0.9659, 0.8178
Data/restraints/parameters	3440/4/290	3440/0/217	6281/0/499
G.O.F. on <i>F</i> <sup>2</sup>	1.039	1.092	0.962
<i>R</i> [ <i>I</i> > 2σ( <i>I</i> )]	<i>R</i> <sub>1</sub> = 0.0328, <i>wR</i> <sub>2</sub> = 0.0746	<i>R</i> <sub>1</sub> = 0.0313, <i>wR</i> <sub>2</sub> = 0.0847	<i>R</i> <sub>1</sub> = 0.0480, <i>wR</i> <sub>2</sub> = 0.0903
$\Delta\rho$ <sub>max/min</sub> . [e Å <sup>-3</sup> ]	0.310/-0.271	0.297/-0.402	0.472/-0.455

ding on the parent C atom. Molecular graphics were prepared using the programs ORTEP3<sup>[21]</sup> and Schakal.<sup>[22]</sup> A summary of the crystal data, structure solution and refinement is given in Table 3.

CCDC-693275 (for **1**), -693277 (for **3**) and -693278 (for **5**) contain the supplementary crystallographic data for this publication. The data can be obtained free of charge from The Cambridge Crystallographic Data Centre via [www.ccdc.com.ac.uk/data\\_request.cif](http://www.ccdc.com.ac.uk/data_request.cif).

**Magnetic Measurements:** Magnetic susceptibility was measured over the range 4–300 K using a longitudinal Faraday system (Oxford Instruments) with a 7 T superconducting magnet, under a magnetic field of 5 T and forward and reverse field gradients of 1 T m<sup>-1</sup>. A polycrystalline sample (19.8 mg) was placed inside a previously calibrated thin-wall Teflon<sup>®</sup> bucket. The force was measured with a microbalance (Sartorius S3D-V). Under these conditions the magnetisation was found to be proportional to the applied magnetic field. The paramagnetic susceptibility of **5** was calculated from raw data assuming a diamagnetic contribution estimated from tabulated Pascal constants as  $-7.38 \times 10^{-4}$  emu mol<sup>-1</sup>.

**Supporting Information** (see also the footnote on the first page of this article): Figures showing CV plots of compounds **1** and **2** in CH<sub>2</sub>Cl<sub>2</sub> and of compounds **1** and **5** in THF are presented.

## Acknowledgments

This work was supported by the Portuguese Fundação para a Ciência e Tecnologia under contract PDCT/QUI/64967/2006 and a post-doctoral grant to S. I. G. D. (SFRH/BPD/28688/2006).

- [1] a) M. Almeida, R. T. Henriques in *Handbook of Organic Conductive Molecules and Polymers* (Eds: H. S. Nalwa), John Wiley & Sons, Chichester, **1997**, vol. 1, pp. 87–149; b) V. Gama, R. T. Henriques, G. Bonfait, M. Almeida, S. Ravy, J. P. Pouget, L. Alcácer, *Mol. Crystals Liquid Crystals* **1993**, *234*, 171–178; c) J. S. Brooks, D. Graf, E. S. Choi, M. Almeida, J. C. Dias,

- R. T. Henriques, M. Matos, *Curr. Applied Phys.* **2006**, *6*, 913–918.  
 [2] a) A. W. Graham, P. Day, *J. Chem. Soc., Chem. Commun.* **1995**, 2061–2062; b) H. Kobayashi, A. Kobayashi, P. Cassoux, *Chem. Soc. Rev.* **2000**, *29*, 325–333.  
 [3] E. Coronado, J. R. Galan-Mascaros, C. J. Gomez-Garcia, V. Laukhin, *Nature* **2000**, *408*, 447–449.  
 [4] L. Balicas, J. S. Brooks, K. Storr, S. Uji, M. Tokumoto, H. Tanaka, H. Kobayashi, A. Kobayashi, V. Barzykin, L. P. Gor'kov, *Phys. Rev. Lett.* **2001**, *87*.  
 [5] a) C. Jia, D. Zhang, Y. Xu, H. Hu, D. Zhu, *Synth. Met.* **2003**, *132*, 249–255; b) N. Bendellat, Y. Le Gal, S. Golhen, A. Gouasmina, L. Ouahab, J. M. Fabre, *Eur. J. Inorg. Chem.* **2006**, 4237–4241; c) J. D. Wallis, J.-P. Griffiths, *J. Mater. Chem.* **2005**, *15*, 347–365.  
 [6] a) Y. Xu, D. Zhang, H. Li, D. Zhu, *J. Mater. Chem.* **1999**, *9*, 1245–1249; b) F. Iwarhori, S. Golhen, L. Ouahab, R. Carlier, J.-P. Sutter, *Inorg. Chem.* **2001**, *40*, 6541–6542; F. Setifi, L. Ouahab, S. Golhen, Y. Yoshida, G. Saito, *Inorg. Chem.* **2003**, *42*, 1791–1793; c) K. Herve, Y. Legal, L. Ouahab, S. Golhen, O. Cador, Y. Yoshida, G. Saito, *Synth. Met.* **2005**, *153*, 461–464; d) A. Ota, L. Ouahab, S. Golhen, O. Cador, Y. Yoshida, G. Saito, *New J. Chem.* **2005**, *29*, 1135–1140; e) L. Wang, B. Zhang, J. Zangh, *Inorg. Chem.* **2006**, *45*, 6860–6863; f) M. Chahma, N. Hassan, A. Alberola, H. Stoeckli-Evans, M. Pilkington, *Inorg. Chem.* **2007**, *46*, 3807–3809; g) M. Moshimann, S.-X. Liu, G. Labat, A. Neels, S. Decurtins, *Inorg. Chim. Acta* **2007**, *360*, 3848–3854; h) Q. Zhu, Y. Lu, Y. Zhang, G. K. Bian, G.-Y. Niu, J. Dai, *Inorg. Chem.* **2007**, *46*, 10065–10070.  
 [7] J. Becher, A. Hazell, C. J. McKenzie, C. Vestergaard, *Polyhedron* **2000**, *19*, 665–672.  
 [8] a) E. Cerrada, C. Diaz, M. C. Diaz, M. B. Hursthouse, M. Laguna, M. E. Light, *J. Chem. Soc., Dalton Trans.* **2002**, *6*, 1104–1109; b) N. Avarvari, D. Martin, M. Fourmigue, *J. Organomet. Chem.* **2002**, *643–644*, 292–300; c) B. W. Smucker, K. R. Dunbar, *J. Chem. Soc., Dalton Trans.* **2000**, *8*, 1309–1315.  
 [9] S.-X. Liu, S. Dolder, E. B. Rusanov, H. Stoeckli-Evans, S. Decurtins, *C. R. Chim.* **2003**, *6*, 657–662.  
 [10] M. Chahma, N. Hassan, A. Alberola, H. Stoeckli-Evans, M. Pilkington, *Inorg. Chem.* **2007**, *46*, 3807–3809.

- [11] A. M. Madalan, C. Rethore, N. Avarvari, *Inorg. Chim. Acta* **2007**, *360*, 233–240.
- [12] a) S. Bouguessa, A. Gouasmia, S. Golhen, J.-M. Fabre, *Tetrahedron Lett.* **2003**, *44*, 9275–9278; b) T. Devic, N. Avarvari, P. Batail, *Chem. Eur. J.* **2004**, *10*, 3697–3707.
- [13] T. Ishida, T. Kawakami, S.-I. Mitsubori, T. Nogami, K. Yamagushi, H. Iwamura, *J. Chem. Soc., Dalton Trans.* **2002**, 3177–3186.
- [14] C. Wang, A. S. Batsanov, M. R. Bryce, J. A. K. Howard, *Synthesis* **1998**, 1615–1617.
- [15] S. Rabaça, M. C. Duarte, I. C. Santos, M. Fourmigue, M. Almeida, *Inorg. Chim. Acta* **2007**, *360*, 3797–3801.
- [16] G. M. Sheldrick, *SADABS*, Bruker AXS Inc., Madison, Wisconsin, USA, **2004**.
- [17] Bruker, SMART and SAINT, Bruker AXS Inc., Madison, Wisconsin, USA, **2004**.
- [18] A. Altomare, M. C. Burla, M. Camalli, G. Cascarano, G. Giacovazzo, A. Guagliardi, A. G. G. Moliterni, R. Spagna, *J. Appl. Crystallogr.* **1999**, *32*, 115–119.
- [19] G. M. Sheldrick, *SHELXL97, Program for Crystal Structure Refinement*, University of Göttingen, Germany, **1997**.
- [20] L. J. Farrugia, *J. Appl. Crystallogr.* **1999**, *32*, 837–838.
- [21] L. J. Farrugia, *J. Appl. Crystallogr.* **1997**, *30*, 565.
- [22] E. Keller, *J. Appl. Crystallogr.* **1989**, *22*, 12–22.

Received: July 1, 2008

Published Online: September 11, 2008